

# Unveiling Short-Term Dynamic of Urban Areas with Airborne LiDAR Data for Change Detection

Wei Yao<sup>\*a</sup>, Stefan Hinz<sup>b</sup>, Uwe Stilla<sup>a</sup>

<sup>a</sup>Photogrammetry and Remote Sensing, Technische Universitaet Muenchen, Arcisstr. 21, 80333, Munich, Germany;

<sup>b</sup>Remote Sensing and Computer Vision, Universitaet Karlsruhe, Englerstr. 7, 76131, Karlsruhe, Germany

## ABSTRACT

Currently, as modern airborne small-footprint laser scanners (airborne LiDAR) are increasingly employed for various urban applications, e.g. building reconstruction, 3d city modeling and planning. Change detection for urban areas using LiDAR technique, which mainly served for damaged building assessment after unforeseen disasters, city ecology monitoring, etc, has been also entered into the scope of research. In contrast to common change detection tasks where the observed events span a long time range, the short-term dynamic refer to those events which frequently happen within a small temporal scale and are not easy and reliable to be detected by long-period observations. The short-term dynamical events have also become represent one of most important elements of urban changes and plays a key role in many applications.

In this paper, we will propose approaches for detecting the short-term dynamic in view of change detection. To test and verify our approaches, multi-aspect airborne LiDAR data within a short revisiting interval and one-path LiDAR data, both of which are acquired over densely built-up areas, are applied respectively. For the multi-aspect data, we mainly deal with the anomaly events happing between every two revisiting flights. Then, it has to be distinguished between view-induced variants and real ones due to the acquisition setting of laser scanning. A spatial-context based height differencing method is introduced to describe and find the changed regions on the co-registered gridded surface. For the one-path data, the moving objects appearing in the urban traffic are our major issue. The scanning mechanism of airborne LiDAR leads to the motion artifacts for instantaneously moving vehicles. Our idea is to make use of this effect to classify the dynamical status of vehicles. The obtained results of experiments using simulated and real data showed us the feasibility and promising of the proposed approaches. Finally, this paper is concluded with present troubles and future works.

**Keywords:** Airborne LiDAR, Urban areas, Change Detection, Short-term, Motion

## 1. INTRODUCTION

Change detection is one of the most important research areas of the remote sensing technology. Timely and accurate change detection of Earth's surface features provides the foundation for better understanding relationships and interactions between human and natural phenomena. It finds important applications within different contexts, ranging from video surveillance to tracking of moving objects, motion estimation, and map update <sup>[1]</sup>. Generally, change detection in remote sensing involves the analysis of multi-temporal datasets from the same geographical area obtained at two different times to quantitatively analyze the temporal effects of the phenomenon. Such an analysis usually aims at identifying large-scale changes that have impressed the sensed ground surface strongly between the two times considered. A variety of change detection techniques have been developed in last decades, however there are so far no universally optimal algorithm for all specific change detection projects <sup>[1][2]</sup>. Several object-based algorithms <sup>[3][4]</sup> including contextual information and pixel region properties such as shape have been proposed to overcome the drawbacks of classical pixel-based approaches due to increasing availability of high resolution image data.

The airborne laser scanning (ALS) has been recently emerging as a powerful technique to explicitly acquire dense and accurate 3d information of Earth's surface independent of lighting conditions. It allow us to simply determine changed regions directly based on comparing the laser points in an inherently consistent planimetric and vertical framework, accordingly avoiding major geometric obstacles for change detection generated by common imaging sensors. Hence, airborne LiDAR has been successfully applied to various practical fields in view of detecting geometric changes, such as costal studies, hydrology and vegetation monitoring <sup>[5]</sup>. Meanwhile, urban areas have

---

\* zhaolingli\_csu@126.com; phone: 13887387600

undergone an active and rapid expansion in last decades and might place great demands on change detection tasks. One of most frequently addressed tasks of change detection using LiDAR data is with respect to building. This kind of application is usually oriented at damaged building assessment as result of natural disaster or examining building detection for updating maps and city planning [6][7]. However, changed buildings, according to our opinion, represent only a portion of dynamical progress in urban areas, i.e. long-term dynamic that usually occurs within a large temporal scale or after unexpected events.

This paper is to address issues of detection of short-term dynamic in urban areas based on the framework of change detection. In contrast to common change detection tasks where the observed events span a long time range, short-term dynamic refer to those events which frequently happen within a small temporal scale and are not easy and reliable to be detected by long-period observations. As indicated by several related research fields [8][9], the short-term dynamical events have become represent an important element of urban changes, such as abnormal activities, human events in open areas and traffic flow, these information typically play a key role in city modeling, security inspection, urban pollution estimation or facility management. The structure of this article is organized into two main parts, with respect to the used data type, i.e. multi-path airborne LiDAR data in section 2 and one-path airborne LiDAR data in section 3. Two approaches based on height context differencing and vehicle motion indication, respectively, will be presented to deal with two datasets by taking the data characteristics into account.

## 2. MULTI-PATH AIRBORNE LIDAR DATA

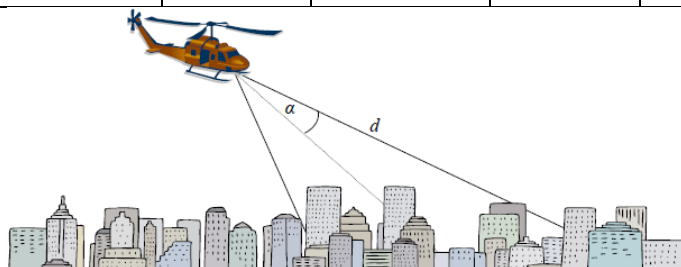
This section is to reveal short-term dynamical events which represent one of most important category of urban changes. We will address an approaches proposed to detect changes in urban areas based on the co-registered airborne LiDAR data of the same site, which are acquired within the same day from four different aspect angle. A spatial-context based height differencing method is introduced to find the characterized regions, where the Bayesian decision theory with Gaussian mixture distribution model is utilized to determine the threshold.

### 2.1 Study data

The study data were recorded by a commercial airborne laser scanner-RIEGL LMS-Q560 equipped with an APPLANIX POS AV over a densely built-up area. The APPLANIX POS AV comprises a GPS receiver and a gyro-based inertial measurement unit (IMU), which is the core element of the navigational system. The GPS data are used for drift compensation and geo-referencing, whereas the IMU determines accelerations with high precision. The laser scanner makes use of the time-of-flight distance measurement principle with nanosecond infrared pulses, giving access to the full waveform by digitizing the echo signal. Opto-mechanical beam scanning provides single scan lines, where each measured distance can be geo-referenced according to the position and orientation of the sensor. Waveform analysis can contribute intensity and pulse-width as additional features, which is typically done by fitting Gaussian functions to the waveforms. Since we are mainly interested in fast processing of the range measurements, we neglect full waveform analysis throughout this paper due to the lack of appropriate calibration of physical reflections. The original physical reflection (e.g. intensity and pulse-width) are usually very sensitive to the variety of acquisition conditions. Four LiDAR datasets are obtained by four flyovers along the different flight paths in an oblique-view - forward-looking scanning mode. The acquisition configurations of this surveying campaign are illustrated in Fig. 1.

Table. 1. LMS-Q560 LiDAR data characteristics and sensor position information of used datasets.

Acquisition date	Swath width(m)	Point density	Fight height(m)	Acquisition time (GMT)	View angle	Aspect angle
23 Sep 2006	420	1.84	420	08:26:31-33	45°	80°
23 Sep 2002		1.56		08:48:21-23		260°
23 Sep 2002		1.75		09:36:31-33		170°
23 Sep 2002		1.85		10:02:51-53		350°



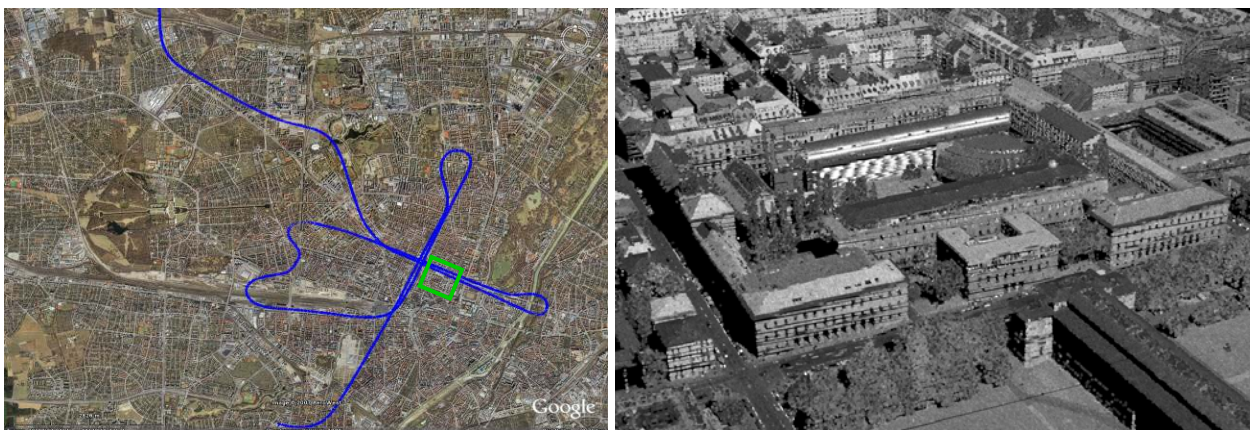


Fig. 1. Top: schema of data acquisition <sup>[10]</sup>,  $a$ : scan angle,  $d$ : sensed range; bottom left: Flight trajectory (blue curves) overlaid with satellite image of the urban region, green box signifies the test site scanned four times from different aspect angles; Bottom right: data sample acquired by the third flyover.

## 2.2 Co-registration

As we all know, a necessary preprocessing step for all change detection algorithms is accurate data registration, the alignment of several datasets into the same coordinate frame. The ICP (Iterative Closet Point) algorithm [11] is most widespread method used to efficiently register 3d shape data. In this work we only consider the registration of two point sets. In literature usually one point set is seen as “data” and the other as “model”. It is assumed that both data sets are approximately in the same position, which is the case for our data. During the ICP operation the whole data shape  $D$  is iteratively moved to be in best alignment with the model  $M$ . The first step of each iteration is to find the closest point  $m$  in  $M$  for each data point  $d$  in  $D$ . The identification of closest points between  $D$  and  $M$  should be accomplished by an efficient method. The result of this step is a sequence  $(m_1, m_2, \dots, m_n)$  of closest model points to all  $n$  data points in  $(d_1, d_2, \dots, d_n)$ . The next step of each iteration is to find a translation and a rotation that moves the data points closest to their corresponding model points, such that the average squared (Euclidean) distance is minimized. This problem can be solved explicitly by the use of quaternions or singular value decomposition.

This work used a modified version of ICP algorithm following the ideas in [10] to co-register every two LiDAR datasets. The basic idea behind them is to filter the different point clouds to get only those points that are most promising to lead to correct correspondences. Therefore, in the first step we want to remove all points belonging to facades of buildings, as their presence in the data sets depends strongly on the viewpoint. It can be done by suppressing all non-maximal laser points falling in each grid cell, in which original 3d information in each cell are stored without interpolation or downsampling. Besides, due to active illumination of the scene by the airborne sensor, most shadows and occlusions occur at the rear of buildings and at ground level. As occlusions are not handled by the ICP algorithm, we need to detect the ground level and remove all points belonging to it. An adaptive thresholding algorithm based on height distribution proposed by [12] is used to find the ground points. It is stated that naturally measured samples (ground points) should lead to a normal distribution according to the central limit theorem. Therefore, by iteratively removing the highest value of the point cloud until the distribution skewness of the height of rest points is balanced, the ground point are supposed to be the rest ones and can then be removed. Yet some clutter objects like vegetation still remain persistent. The next step is to remove these irregular shaped objects. RANSAC is employed to do a robust plan fitting among the points in order to distinguish between man-made and clutter objects. As final results, the building roofs are found with associated points and their corresponding normal vectors (Fig. 2).



Fig. 2. Top view of the point cloud after removing clutter objects. Color coded map according to the estimated normal <sup>[10]</sup>.

Now that we have removed all data that might lead to an incorrect registration, we start to proceed with the normal ICP procedure. After the search for corresponding points by defining suitable distance measures,  $M$  and  $D$  are translated to the origin by  $c_m$  and  $c_d$ , respectively:

$$\begin{aligned} \overline{M} &= \{\overline{m}_i \mid \overline{m}_i = m_i - c_m, i = 1, \dots, n\} \\ \overline{D} &= \{\overline{d}_i \mid \overline{d}_i = d_i - c_d, i = 1, \dots, n\} \end{aligned} \tag{1}$$

where  $c_m$  and  $c_d$  are centroids of all points among the set of  $n$  correspondences are computed.

$$\begin{aligned} H &= \sum_{i=1}^n \overline{d}_i \overline{m}_i^T \\ R &= VU^T, \quad t = c_m - Rc_d \end{aligned} \tag{2}$$

The singular value decomposition  $H = UAV^T$  of this  $3 \times 3$  matrix  $H$  leads to the optimal rotation  $R$  and translation  $t$ . Afterwards, we transform the data set  $D$  with respect to  $R$  and  $t$  and continue with the next ICP iteration until a stop criterion is met. Once every two datasets of LiDAR points are brought in a consistent geometric framework, they will be further transformed into the gridded surface data (Fig.3) for generating change detection map.

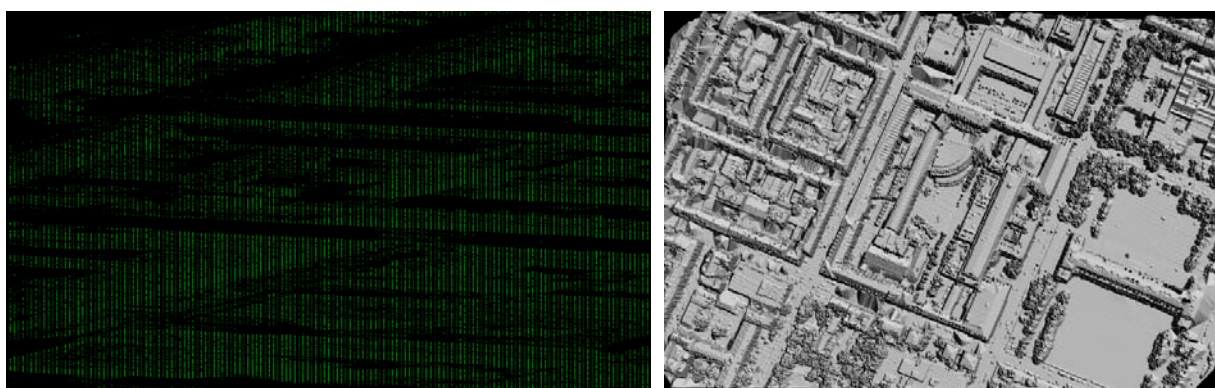


Fig. 3. An example of co-registered LiDAR data, two datasets were acquired by first and second flyover. Left: point cloud; Right: gridded surface

### 2.3 Change detection based on height differencing map

In this section, the first step is to generate a temporal difference image from two co-registered gridded LiDAR range data. The second step is to identify and extract areas or features that may have changed from the difference image by employing the contextual Bayesian decision method

Early change detection methods were based on yielding the signed temporal difference image  $D(X) = L_1(X) - L_2(X)$ , and such approaches are still widespread. The most obvious algorithm is “simple differencing”, namely threshold the difference image to generate the change mask according to the following decision rule:

$$B(X) = \begin{cases} 1, & \text{if } |D(X)| > \tau \\ 0, & \text{otherwise.} \end{cases} \tag{3}$$

Often, the threshold is chosen empirically. However the threshold is chosen, simple differencing with a global threshold is unlikely to outperform the more advanced algorithms in real-world applications. This technique is sensitive to noise and does not consider local consistency properties of the change. Therefore, we present a more sophisticated algorithm for our application based on spatial-context in Laser point cloud. It exploits the close relationships between nearby points in space by fitting the height values of each block to a polynomial function of the grid position coordinates. In two dimensions, this corresponds to

$$\hat{H}_k(x, y) = \sum_{i=0}^p \sum_{j=0}^{p-i} \beta_{ij}^k x^i y^j \tag{4}$$

where  $p$  is the order of the polynomial model. It has been concluded by [13] that the quadratic model is generally superior to others. So we suggested a test statistic that involved spatial partial derivatives of the quadratic model, given by

$$T(X) = \sum_{P \in \Omega_x} \left( \frac{\partial \hat{H}}{\partial x}(P) + \frac{\partial H}{\partial y}(P) \right) \tag{5}$$

to serve as feature value delivered to generating the differencing map. Using this value can make the change detection of LiDAR independent of linear variations in height value and more reliable against anomalies present in the local neighborhood.

After a difference image is created from bi-temporal gridded LiDAR data, the extraction of changed areas could be considered as a classification problem between two categories: changed versus unchanged. The thresholding scheme does provide a simple and practical way to identify changed areas in spite of some inherent limitations. To tackle complexity of real LiDAR data resulting in a large deviation in estimated threshold, a method based on the Bayes Rule of Minimum Error (BRME) for threshold determination [14] is applied. The distribution of height values in the differencing model is modeled as mixture of two classes, i.e., changed (denoted as  $\omega_c$ ) and unchanged (denoted as  $\omega_n$ ), and each class is assumed to be subject to a Gaussian mixture distribution model. Then, distribution parameters, comprising means, standard deviations, and *a-priori* probabilities, are estimated from the LiDAR by employing Expectation- Maximization (EM) algorithm, and the threshold  $T$  should be a sound solution to following equation of  $X$ :

$$P(\omega_c)P(X | \omega_c) = P(\omega_n)P(X | \omega_n) \tag{6}$$

where  $P(\omega_i)$  and  $P(X | \omega_i)$  are a priori probability and class conditional probability of class  $i$  ( $i = n, c$ ), respectively. The Gaussian mixture distribution model assumes distribution of each class to be a mixture of several Gaussian components, expressed as

$$f(X) = \sum_{i=1}^r w_i f_i(x) \tag{7}$$

where  $r$  is the number of Gaussian components,  $f_i(x)$  is the PDF for the  $i$ th Gaussian component, and  $w_i$  is the non-zero weight for the  $i$ th Gaussian component that satisfies normalization condition: i.e.  $\sum_{i=1}^r w_i = 1$

### 2.4 Results and visual assessment

To keep the detected changes consistent with as possible, the proposed algorithm is applied to every two datasets of studied LiDAR data captured by four flyovers, both of which are scanned along the opposite directions, e.g. flyover 1 and 2. The results for first and second flyovers are illustrated in Fig.4. Since the “ground-truth” data for the changed objects or regions in our case are too difficult to obtain, the results are first examined empirically by a visual analysis. It can be perceived that in spite of applying the LiDAR data scanned parallelly for the test, major detected changes in urban areas correspond to faked geometric changes due to oblique view of laser scanner, such as shadow areas next to high buildings and tree canopies. Nevertheless, another important element of dynamic which happens within such a small temporal scale concentrates on traffic-related objects and can be observed in the resulted change detection map. They could appear in roads, parking lots or inner yards which usually characterize many human activities. The feasibility of using airborne LiDAR to reveal substantial events in urban areas can be said to be ensured if the sensor and acquisition geometry –induced effects are to be effectively distinguished.

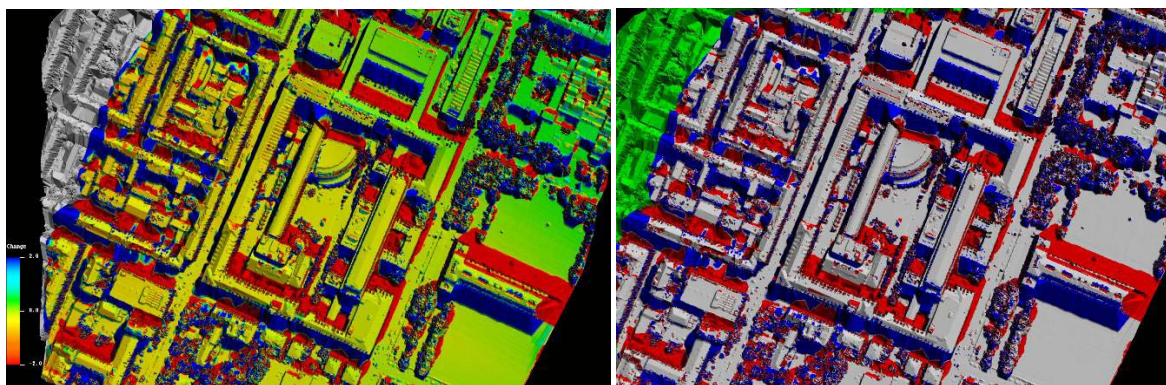


Fig. 4. Change detection results for first and second flyover. Left: change detection map, the severity of change is highlighted by a continuous color palette scaled from -2.0m to +2.0m; Right: detected changed regions beyond the determined threshold, Red regions are lower than the comparison model while blue ones are higher, green indicate regions where models are not overlapped.

### 3. ONE-PATH AIRBORNE LIDAR DATA

This section is to address the problem of extracting dynamical information directly from one-path airborne LiDAR data. Since the acquiring time interval of this kind of dataset is very short, the moving objects appearing in the urban traffic are our issue here and represent the major dynamic. The model for moving vehicle in the airborne LiDAR data is to be defined and exploited. The single vehicles can be extracted as point sets and then classified in terms of their movement status based on the shape analysis. In principle, the velocity might also be estimated by inverting the shape distortion when the prerequisite is met.

#### 3.1 Moving vehicle model

For the purpose of better understanding of sensor mechanism and data characteristics, it is assumed that the vehicle modeling is equally required for vehicle detection in the context of traffic monitoring from airborne LiDAR, in spite that the consistent object modeling in the ALS data is very difficult.

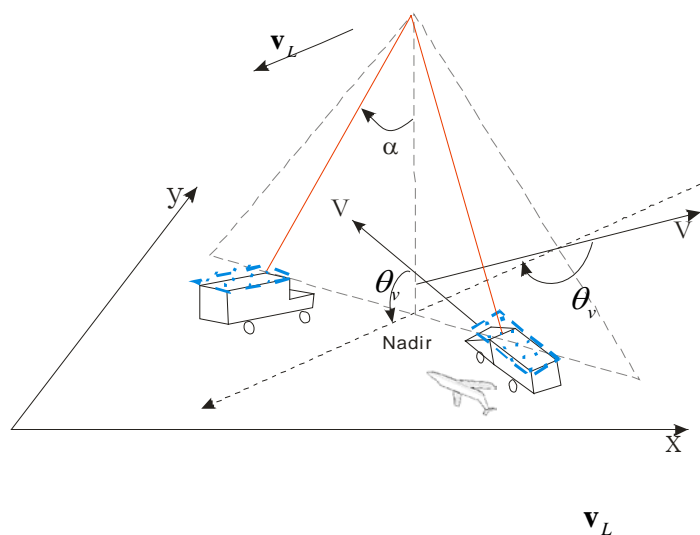
The moving vehicle here refers to the instantaneous moving cars when the scanning pattern sweeps over them. This category comprises the essential part of dynamical information for traffic flow analysis while another part of traffic dynamics caused by temporally motionless vehicles were considered before in multi-path LiDAR data .

The fundamental difference between scanning and the frame camera model, with respect to the moving objects, is the presence of motion artifacts in the scanner data [15]. The frame imagery preserves the shape of the moving objects because of the relatively short sampling time (camera exposure). But if the relative speed between the sensor and the object is significant, the motion blurring may increasingly occur. Contrarily, the scanning mechanism always produces motion artifacts; moving objects will be deformed and have a different shape in the recorded data, depending on the relative motion between the sensor and the object and sampling frequency. Usually in the laser scanning data, the moving object would be projected as stretched, compressed or skewed compared to the original one and its 2D shape distortion can be summarized in Eq.8. Fig. 5 depicts the mutual relationships of moving vehicle under ALS and an example in the simulated laser data.

$$l_s = \frac{l_v \cdot |\mathbf{v}_L|}{|\mathbf{v}_L| - |\mathbf{v}| \cdot \cos(\theta_v)} \tag{8}$$

$$\alpha_v = \arctan \left( \left( \frac{w_v \cdot \sin(\theta_v)}{|\mathbf{v}_L| - |\mathbf{v}| \cdot \cos(\theta_v)} \right) \cdot |\mathbf{v}| \cdot \frac{1}{w_v} \right)$$

where  $\theta_v$  : angle between the flight path and the vehicle trajectory;  $\mathbf{v}$  : vehicle velocity;  $\mathbf{v}_L$  ,  $v_{l-long}$  ,  $v_{l-long}$  : laser scanner velocity and its across- and along-track component;  $l_s$  : sensed vehicle length;  $l_v$  : true vehicle length;  $w_v$  : true vehicle width;  $\alpha_v$  : skewing angle of vehicle form, angle of parallelogram deformed vehicle shape.



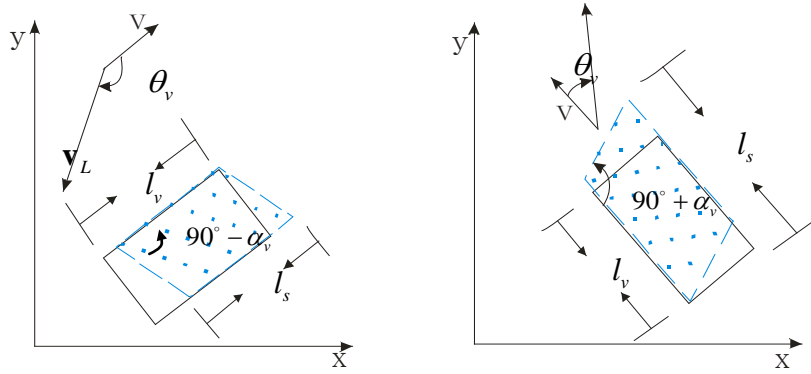


Fig. 5. Moving vehicle in the ALS data, top: schematic description of mutual relations, bottom: top-view for situations having different relative moving directions, blue indicates sensed vehicle object.

Generally, a vehicle is assumed to be a rectangle surface in the object space. Following conclusions can be obtained from the simulation results: the along-track ( $\theta_v = 0^\circ/180^\circ$ ) motion leads to stretch or shrink of the vehicle length ( $l_s$ ) in the scanning data, whereas the across-track motion ( $\theta_v = 90^\circ/270^\circ$ ) leads to skewing ( $\alpha_v$ ) of the vehicle shape. Therefore, for the most cases the vehicle will appear as deformed parallelogram in the scanning data – combination of both motion effects. In principle the shape deformation of the vehicle can be used to quantitatively derive the movement status, but a prerequisite must be fulfilled that the true vehicle length is known. And its accuracy and sensitivity depend strongly on various impact factors, such as point density, horizontal position errors, or reflection properties of surface material.

### 3.2 Vehicle detection

In this subsection we will briefly address the approach to extract the vehicles from ALS data, which were developed in [16]. It is assumed that regardless of the movement status firstly, the vehicle points should be extracted as complete as possible. The extraction strategy comprises knowledge about how and when certain parts of the vehicle and context model are optimally exploited, thereby forming the basic control mechanism of the extraction process. In contrast to other common approaches dealing with LiDAR data analysis, we neither use the reflected intensity for extraction nor we combine multiple data sources acquired simultaneously as, e.g. [15] or [17] do, to support vehicle extraction. Our philosophy is to exploit geometric information of ALS data as much as possible and to extract vehicle objects from each original strip separately. We believe that the geometric feature is of great significance within the interpretation of ALS data, since it imposes considerably strong constraints on object relations and is recorded and represented directly and explicitly. Moreover, the approach on one side can be viewed as a progressive bottom-up strategy and on the other side is a straightforward method being in accordance with human inference. The method is subdivided into four main steps that are summarized in a flowchart in Fig. 6.

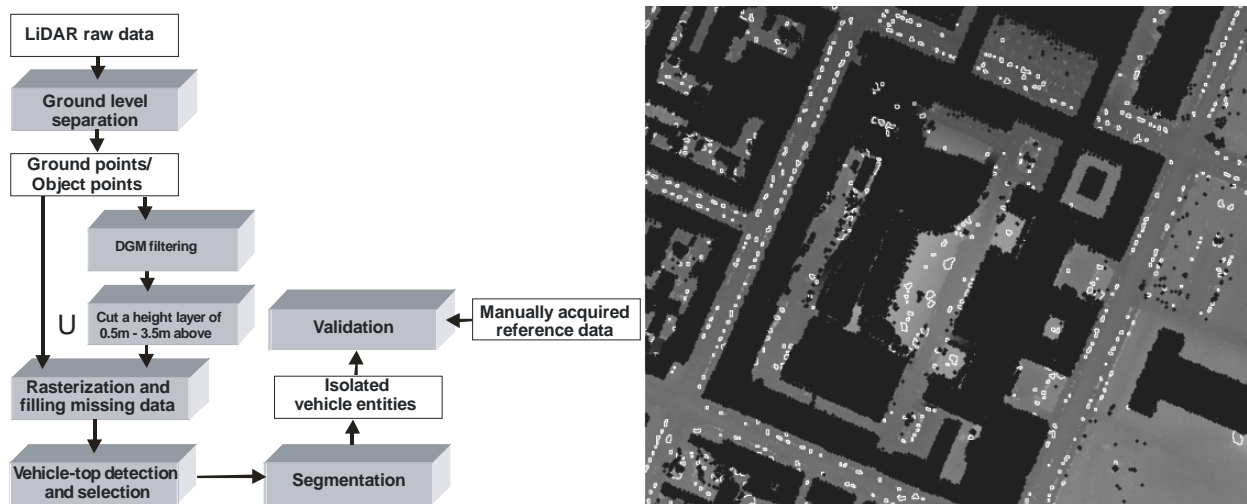


Fig. 6 Left: workflow of the vehicle detection approach; Right: an example of vehicle detection result from airborne LiDAR data

Finally, the extracted vehicles (Fig. 6) with delineated contours can serve as an adequate clue to accurate determination of object extent in the raw LiDAR data, thereby enabling the modeling and parametrization of vehicle shape in 3d point cloud for motion analysis.

### 3.3 Vehicle motion analysis based on simulated and real data

After single vehicles are extracted by last step, the delineated contour of each vehicle can further be delivered to the task of analyzing the movement status by shape analysis of point sets. In order to illustrate this effect we also have designed an ALS simulator for demonstrating and validating the appearance of moving object in ALS data according to sensor and geometric parameters during the data acquisition. The riegL LMS-Q560 scanner was used to acquire the test data whose data characteristics and sensor position information. The simulator will adopt the same data as input parameters. Our test is meant to focus on car travelling in urban roads, vehicle is assumed to have a true length of about 3.5m. Three different examples of moving vehicle in ALS data with respect to the motion mode i.e. along-track motion, across-track motion and curved motion are chosen here to demonstrate the feasibility and potential of the established model(sec.3.1) for moving vehicle (Fig. 7), the estimated velocities are then to be compared and validated with corresponding simulated scenarios. The results can be accessed in Table. 2 in respect of form consistence.

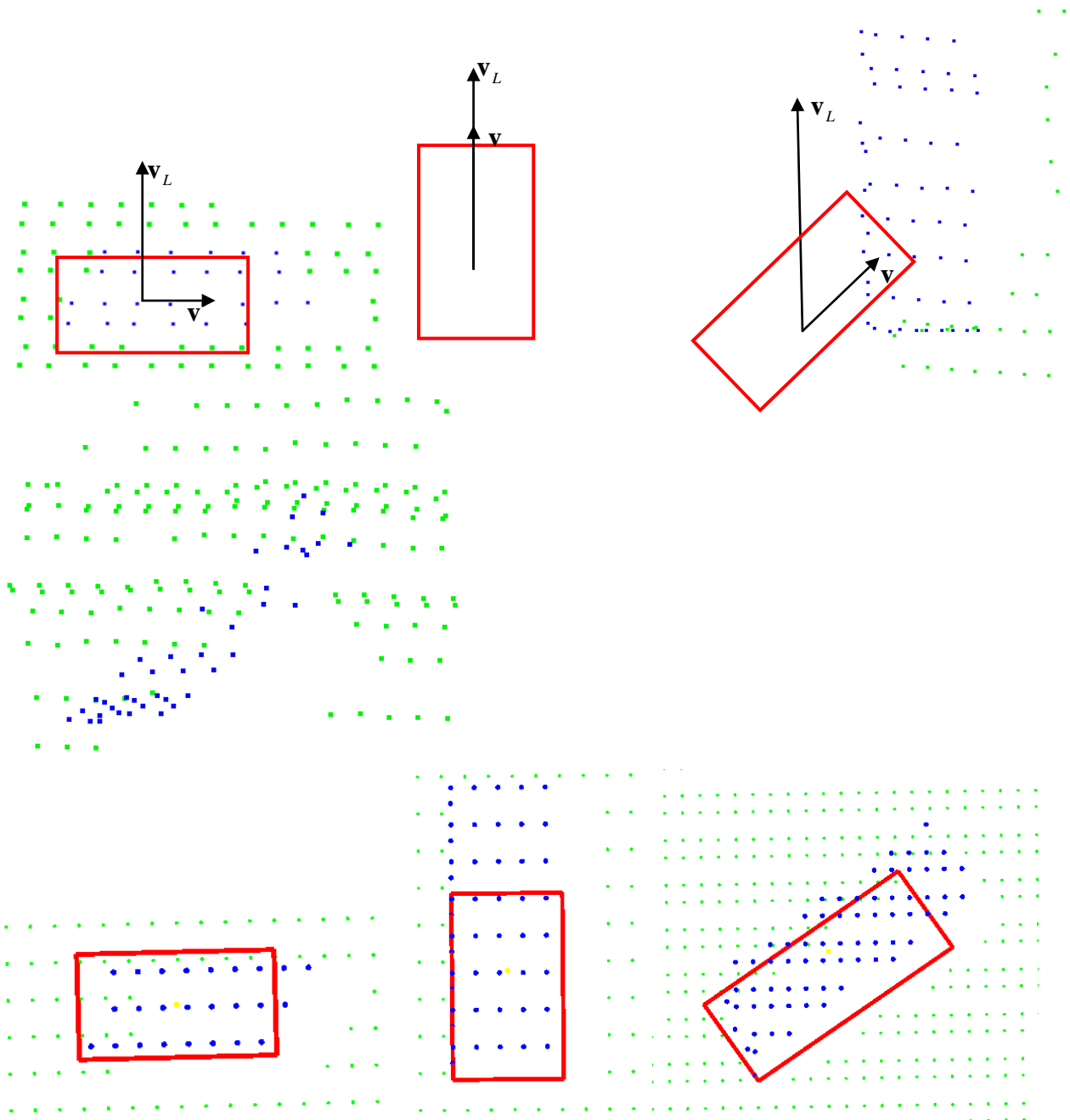


Fig. 7. Three cases of motion indication and velocity estimation for vehicle. Left: along-track motion; Middle: across-track motion; Right: curved motion. Top: real LiDAR data; Bottom: simulated data using estimated velocity and assumed vehicle size. Blue points: vehicle points, green points: ground points, red box: original vehicle outline.

Table. 2. Vehicle velocity estimation comparison between real and simulated data.

Vehicle number	Vehicle velocity derived from assumed vehicle length measurements [m/s]	Comparison with simulated scenarios
	Using vehicle class length (3.5m )	Using the derived velocity and assumed vehicle size
1.	18.35	Less high form conformity
2.	13.84	High form conformity
3.	10.13	Low form conformity, ambiguous surface reflection

#### 4. CONCLUSIONS

In this work, airborne LiDAR data were analyzed in view of revealing the short-term dynamic in urban areas for change detection. Two kinds of LiDAR dataset, i.e. multi-path and one-path data, were used to detect changes happening within two different temporal scales. A change detection method by exploiting spatial neighborhood in co-registered LiDAR differencing height grid and a motion indication method based on shape analysis of point sets are presented to deal with dynamical objects in two LiDAR data sets, respectively. The preliminary results have shown us feasibility and high potential of airborne LiDAR towards discovering the various changed events in urban areas of broad coverage. Nevertheless, there are meanwhile some deficiencies of the proposed approaches needed to be handled in future work. For multi-path dataset, we need to distinguish fake changes induced by LiDAR scanning geometry from real ones caused by real progress such as anomaly events, traffic movement. For one-path data, Application-specific vehicle length has to be predefined. The estimated velocity of moving vehicles could be averaged for a broadly observed area, so as to obtain a statistically accurate result in view of deriving traffic flow parameters.

#### REFERENCES

[1] Lu, D., Mausel, P., Brondizio, E. and Moran, E., "Change detection techniques, "International Journal of Remote Sensing, 25(12), pp.2365 - 2401(2004).

[2] Tian, M., Wan, S. and Yue, L. "A Novel Approach for Change Detection in Remote Sensing Image Based on Saliency Map, "In Proceedings of the Computer Graphics, Imaging and Visualisation. IEEE Computer Society, Washington, DC, 397-402(2007).

[3] Walter, V., "Object-based classification of remote sensing data for change detection, "ISPRS Journal of Photogrammetry and Remote Sensing, 58(3-4), pp. 225-238(2004).

[4] Im, J., Jensen, J. R. and Tullis, J. A., "Object-based change detection using correlation image analysis and image segmentation," International Journal of Remote Sensing, 29(2), pp.399 -423(2007).

[5] Streutker, D., "Change Detection with LiDAR Data," LiDAR Littoral Studies Workshop, Monterey, California (2007).

[6] Vosselman, G., Gorte, B.G.H. and Sithole, G., "Change detection for updating medium scale maps using laser altimetry," International Archives of Photogrammetry, Remote Sensing and Spatial Information Sciences, vol. 34, part B3, Istanbul, Turkey, July 12-23, pp. 207-212(2004).

[7] Murakamia, H., Nakagawaa, K., Hasegawaa, H., Shibatab, K. and Iwanami, E., "Change detection of buildings using an airborne laser scanner, "ISPRS Journal of Photogrammetry and Remote Sensing, 54(2-3), pp. 148-152(1999).

[8] Yao, W., Hinz, S., and Stilla., U., "Traffic monitoring from airborne LiDAR - feasibility, simulation and analysis, "XXI Congress, Proceedings. International Archives of Photogrammetry, Remote Sensing and Spatial Geoinformation Sciences, Vol 37(B3B):593-598(2008).

[9] Zeibak, R. and Filin, S., "Change Detection via Terrestrial Laser Scanning, " ISPRS Workshop on Laser Scanning 2007 and SilviLaser 2007, Espoo, Finland, 430-435(2007).

[10] Hebel, M. and Stilla, U., "Automatic Registration of Laser Point Clouds of Urban Areas," PIA07 Photogrammetric Image Analysis 2007. International Archives of Photogrammetry, Remote Sensing and Spatial Geoinformation Sciences, Vol 36(3/W49A) 13-18(2007).

[11] Besl, P. J. and McKay, N. D., "A method for registration of 3-D shapes, " IEEE Transactions on Pattern Analysis and Machine Intelligence, Vol. 14, No. 2, pp. 239-256(1992).

- [12] Bartels, M., Wei, H. and Mason, D.C., "DTM Generation from LIDAR Data Using Skewness Balancing," Proceedings of 18th International Conference on Pattern Recognition, Hong Kong, Vol(01): 566-569(2006).
- [13] Hsu, Y. Z., Nagel, H. H. and Reckers, G., "New likelihood test methods for change detection in image sequences," *Comput. Vis., Graph. Image Process*, vol. 26, pp. 73-106(1984).
- [14] Zhang, L., Liao, M. S., Yang, L. M. and Lin, H., "Remote sensing change detection based on canonical correlation analysis and contextual Bayes decision," *Photogrammetric Engineering and Remote Sensing*, 73 (3): 311-318(2007).
- [15] Toth, C. K. and Grejner-Brzezinska, D., "Extracting dynamic spatial data from airborne imaging sensors to support traffic flow estimation," *ISPRS Journal of Photogrammetry and Remote Sensing*, 61(3-4): 137-148(2006).
- [16] Yao, W., Hinz, S. and Stilla, U., "Automatic vehicle extraction from airborne LiDAR data of urban areas using morphological reconstruction," *Pattern Recognition in Remote Sensing (PRRS 2008)*, 2008 IAPR Workshop on, pp.1-4, 7-7 (2008).
- [17] Gao, B. and Coifman, B., "A Vehicle Detection and Tracking Approach Using Probe," *Vehicle LIDAR Data. Traffic and Granular Flow'05, Part VI*, pp.675-685(2007).